IRA-International Journal of Applied Sciences
ISSN 2455-4499; Vol.20, Issue 01 (Q.1 2025)
Pg. no. 1-13.
IRA Academico Research

Numerical Study of the Spatial Profiling of Airflow in A Solar Cold Room Filled with Agricultural Products with Validation of The Model Developed

Hermann KABORE [1#], **Roger Mathurin Charles COMPAORE**[1,2], **Kassoum YAMBA**[2], **Kalifa PALM**[1,2], **Oumar SANOGO**[1,2], **Tamba CAMARA**[3], **N'wuitcha KOKOU**[4]

[1]Université Joseph KI-ZERBO, Unité de Formation et de Recherche en Sciences Exactes et Appliquées (UFR-SEA), Laboratoire d'Energies Thermiques Renouvelables (L.E.T.RE), 03 BP 7021 Ouagadougou, Burkina Faso

[2]Centre National de la Recherche Scientifique et Technologique (CNRST), Institut de Recherche en Sciences Appliquées et Technologies (IRSAT), Laboratoire des Systèmes d'Energie Renouvelable et Environnement-Génie de Mécanique Industrielle (LASERE-GMI), 03 BP 7047 Ouagadougou 03, Burkina Faso

[3]Laboratoire Interdisciplinaire des Sciences et Didactique des Sciences (LISDIS), Ecole Normale Supérieur (ENSup) de Bamako-Mali

[4]Laboratoire sur l'Energie Solaire – Groupe Phénomène de Transfert et Energétique (LES-GPTE), Faculté des Sciences, Département de Physique, Université de Lomé, 01BP 1515 Lomé1-Togo.

[#]corresponding author

Type of Work: Peer Reviewed.
DOI: https://dx.doi.org/10.21013/jas.v20.n1.p1

Review history: Submitted: Feb 10, 2025; Revised: March 07, 2025; Accepted: March 20, 2025.

How to cite this paper:
Kabore, H., Compaore, R.M.C., Yamba, K., Palm, K., Sanogo, O., Camara, T., Kokou, N. (2025). Numerical Study of the Spatial Profiling of Airflow in A Solar Cold Room Filled with Agricultural Products with Validation of The Model Developed. *IRA-International Journal of Applied Sciences* (ISSN 2455-4499), 20(1), 1-13. https://dx.doi.org/10.21013/jas.v20.n1.p1

Hermann KABORE /0009-0008-3377-4009

ABSTRACT

The aim of this work is to carry out a numerical analysis of the airflow field in a 3D solar cold room in order to determine the variation in air velocity. The cold room, with external dimensions of 5.10 m×3.00 m×2.60 m, rests on concrete blocks about 40 cm above the ground, creating an empty space. Inside the storage room, crates containing tomatoes were placed on pallets occupying a large volume of this space. A Computational Fluid Dynamics (CFD) simulation study was carried out using COMSOL Multiphysics software, version 5.3a, at constant evaporator unit diffusion airflow. The study showed inhomogeneity of air velocity distribution within the device. However, the middle (Z = 0.91 m) and lower (Z = 0.31 m) planes show a high degree of air velocity uniformity compared with the upper plane (Z = 1.51 m). The air velocity heterogeneity index calculated for the middle and lower planes is 41.64% and 102.90% respectively, compared with 222.06% for the upper plane. An experimental study was carried out to validate the results of the simulation tool. The average relative absolute error of the CFD calculation is 0.31 on the middle plane and 0.15 on the lower plane. This numerical and experimental study is essential for understanding the mechanism of air circulation in cold stores.

Keywords: cold store, air velocity distribution, CFD, velocity heterogeneity index, mean relative error.

Introduction

When the main parameters, such as humidity, temperature and air velocity, are respected in a cold store, the food products preserved during storage retain their original condition once they leave the cold store. This is due to the fact that cold slows down the respiration of agricultural products, delaying their ripening and halting their physiological, biochemical and microbiological deterioration processes. However, the ripening of agricultural crops can be unpredictable due to storage conditions that are difficult to homogenize in cold stores. Numerous studies have shown inhomogeneity in airflow temperature, velocity or humidity in cold rooms (Hoang et al., 2015), refrigerated trucks (Moureh et al., 2002) and domestic refrigerators (Asmi et al., 2013) or in containers (Cardinale et al., 2016). This air inhomogeneity is due to the design of cold stores, the location of evaporator units and/or serpentine conductors, the cooling of internal equipment (pallets, crates, light bulbs, forklifts, scales, etc.) or the breathing of products in the case of a loaded cold room. Other studies confirm the heterogeneity of cooling by showing that in a cold room, the crates containing fruit and vegetables placed near the evaporator unit were subjected to higher air temperatures than the rear crates, resulting in product cooling rates and temperature heterogeneity (Duret et al., 2014). Recent studies by (Bishnoi & Aharwal, 2020) in a cold room showed heterogeneity in air velocity and temperature along the axis and height of the device. The upper and middle planes showed a large vortex that was much more active than the lower planes. Studying the circulation of the airflow is proving difficult for researchers who can't find analytical solutions to this complex geometry. For this reason, the numerically approximated solution is considered an interesting alternative (Amadou Oumarou, 2021).

Computational fluid dynamics (CFD) is a powerful tool for characterizing temperature and air velocity fields in refrigerated warehouses. This tool can be used to solve coupled partial differential equations, such as the Navier-Stokes equations, in which mass, momentum and energy transfers between the air and the products to be stored are described (Lewis et al., 2004). Ansys Fluent, Ansys CFX and COMSOL Multiphysics software (COMSOLMultiphysicsTM, 2007) are used in a number of applications. The latter is a scientific commercial software package for thermofluidodynamic simulations.

Thanks to the evolution of fundamental computer concepts, it is now possible to present airflow models and temperature attributes in an operational cold room. Our study will involve developing a mathematical model of the conservation equation for the fluid's momentum inside the cold device. Emphasis will be placed on the precise measurement of air velocity during experimental tests. The results of the latter will be used to validate the results of the numerical simulation. The average relative absolute error of the CFD calculation is 0.31 in the middle plane and 0.15 in the lower plane.

Materials and Methods

Materials

The parallelepipedic bioclimatic model presented by the authors (KABORE et al., 2024) is used for computational fluid dynamics (CFD) simulation. This monoblock model comprises a technical room and a preservation chamber with external dimensions of 5.10 m×3.00 m×2.60 m. Inside the preservation chamber, crates containing tomatoes were placed on pallets on the floor, as shown in Figure 1 (*see Figures & Tables section*). The preservation chamber is made up of two physically different environments: fluid + “solid” (tomatoes). The spaces between the rows and between the crates form the fluid medium. The tomato bed is assimilated to a porous medium with the pallets and crates in cubic form with a porosity ϵ equal to 41.19% (Uba et al., 2020). A porous medium is defined as a material made up of a solid matrix and “holes” called pores, occupied by a fluid that may be in one or more phases (gas, liquid or gas and liquid), referred to as single-phase or two-phase flow (OUEDRAOGO, 2017).

For air circulation tending towards cooling uniformity in cold stores, three types of rectangular or circular duct evaporator units have been proposed by authors (Sajadiye & Zolfaghari, 2017). These are cold stores with a heat exchanger and ventilation unit, cold stores with a slotted ceiling duct and cold stores with a slotted plenum wall. Our refrigeration circuit model is therefore that proposed by the authors (KABORE et al., 2024), featuring two ventilation units with heat exchanger, each with an air flow rate of 20 m^3/min and 0.06 m^2 of circular duct surface.

Methods

Aeraulic Parameters

Air velocity homogeneity in the produce zone can improve the airflow field inside the cold store. However, the presence of agricultural products disturbs the airflow, which then becomes disordered and heterogeneous. The deviation of air velocity at different positions from the mean velocity illustrates the heterogeneity of the velocity, a phenomenon known as the “air velocity heterogeneity index". Of the latter, the lower its value, the more uniformly the velocity is distributed at the location where it is calculated or measured (Bishnoi & Aharwal, 2020). It is defined as follows:

$$HI = \frac{\sqrt{(u-\bar{u})^2}}{\bar{u}} \times 100 \tag{1}$$

Model Assumption

- Bulk packages of Cobra variety tomatoes in pallet boxes were modeled in cubic form as a porous medium with a heat source, as we assumed that the products contribute heat through respiration and moisture loss due to vapor pressure deficit. Numerous studies have shown that the porous medium model is reliable enough to be applied to large devices such as cold storage facilities (Hoang et al., 2015; Sajadiye & Zolfaghari, 2017);
- The flow is turbulent. The type of turbulence model is RANS (Reynolds-Averaged-Navier-Stokes) and the turbulence model is κ-ε;
- The 3D numerical simulation partly takes, only, the conservation local;
- The fluids composing the porous medium are incompressible;
- The flow is single-phase.

Governing Equations

Airflow Model

Experimental measurements lead us to high Reynolds numbers (Re > 2300), which places us in a turbulent regime. The Reynolds number corresponds to the ratio between inertial and viscous forces, and measures the degree of turbulence in the flow.

$$Re = \frac{VD_H}{\nu} \tag{2}$$

The Navier-Stokes equation, completed by the continuity equation, expresses the conservation of momentum of the fluid, defined as follows (Cardinale et al., 2016):

$$\rho(\mathrm{U}.\nabla)\mathrm{U} = \nabla.\left[-p2I + (\mu+\mu_T)(\nabla U + (\nabla U)^T) - \frac{2}{3}(\mu+\mu_T)(\nabla.U)I - \frac{2}{3}\rho k2I\right] + F \tag{3}$$

$$\rho\nabla.(\mathrm{U}) = 0 \tag{4}$$

Added to this are those relating to the turbulent kinetic energy balance k and the dissipation rate per unit mass ε.

$$\rho(U.\nabla)k = \nabla.\left[\left(\mu + \frac{\mu_T}{\sigma_k}\right)\nabla k\right] + P_k - \rho\varepsilon \tag{5}$$

$$\rho(U.\nabla)\varepsilon = \nabla.\left[\left(\mu + \frac{\mu_T}{\sigma_\varepsilon}\right)\nabla \varepsilon\right] + C_{\varepsilon 1}\frac{\varepsilon}{k}P_k - C_{\varepsilon 2}\rho\frac{\varepsilon^2}{k} \tag{6}$$

$$\mu_T = \rho C_\mu \frac{k^2}{\varepsilon} \tag{7}$$

$$P_k = \mu_T \left[\nabla U.(\nabla U + (\nabla U)^T) - \frac{2}{3}(\nabla . U)^2\right] - \frac{2}{3}\rho k \nabla . U \quad (8)$$

The inlet boundary conditions I_x, defined as turbulent intensity, and L_T, as turbulence length scale, were calculated as follows:

$$I_x = 0{,}16(Re_L)^{-1/8} \quad (9)$$

$$L_T = 0{,}07L \quad (10)$$

The I_x and L_T values were used to calculate k and ε :

$$k_0 = \frac{3}{2}(U_{0x}/I_x)^2 \quad (11)$$

$$\varepsilon_0 = C_\mu{}^{3/4}\frac{k^{3/2}}{L_T} \quad (12)$$

Initial Conditions

A $t = t_0$, he comes :

$U = U_x = U_y = U_z = 0$;

P = Atmospheric pressure

Boundary Conditions

The boundary conditions on speed can be written as :

On evaporator unit output : $U_x = V$; $U_y = U_z = 0$

On all solid surfaces : $U_x = U_y = U_z = 0$

Numerical Resolution

The simulation was carried out on a personal computer equipped with an Intel(R) Core(TM) i5 CPU M 520 @ 2.40GHz 2.40 GHz, with an airflow of 20 m^3/min and a Reynolds number of 64750. COMSOL Multiphysics software, version 5.3a, was used to solve the airflow model using the finite element method. The computational domain was first discretized (subdivided) into a mesh of many small elements. Four-node tetrahedral element meshes were used for the 3D model.

Airflow Model Validation Method

During the experimental tests, quantitative velocity measurements are made using a hot-wire anemometer inside the cold room, as this is a practical procedure and its measurement range is acceptable (0.1 to 20 m/s) with an accuracy of ± 0.05 m/s. Air velocities are measured in two planes along the heights (0.31 m, 0.91 m and 1.51 m) and are referred to as the “bottom plane”, “middle plane” and “top plane” respectively, as shown in Figure 2. Air velocity is measured at 43 points on each plane in the product area.

At each point, the velocity components in the x, y and z directions are measured, assuming that the cylindrical face of the thermo-anemometer sensor reflects the normal velocity component of the airflow from the evaporator unit. The velocity amplitude (u) at each location is calculated as follows:

$$u = \sqrt{v_x^2 + v_y^2 + v_z^2} \tag{13}$$

The results obtained from these experimental tests are used to compare with those of the airflow model in order to validate them.

The error was calculated as the relative mean absolute difference between the measured and calculated velocity amplitude (Nahor et al., 2005):

$$\bar{E}_{CFD} = \frac{1}{N}\sum_{I=1}^{N}\frac{|u|_{CFD}^{I} - |u|_{exp}^{I}}{|u|_{exp}^{I}} \tag{14}$$

Results and Discussion

Velocity Distribution

The unloaded no-load airflow obtained from the CFD porous medium approach, with a diffused air supply and constant flow in the axial direction, is shown in Figure 3. The air flow appears to be homogeneous, from the evaporator unit to the front wall, then back to the air coolers via the floor. The cycle continues in this way until the set temperature is reached.

However, the presence of agricultural produce inside the cold store disturbs the air flow field, making it disordered and non-uniform. Figure 4 illustrates the air velocity distribution on the three XY planes at different heights, as well as the cross-section. Figure 4-d)- shows the flow of air on the ZX plane from its diffusion through the evaporators to its outlet. The air flow is reflected by the front wall, then returns to the coolers via the middle and floor of the device. Figure 4-a)- shows the circulation of air velocity on the upper plane. Cold air diffused from the evaporator unit has caused a high velocity impact in the area next to the front wall. At the rear of the upper plane, part of the return air is drawn in by the cold air blast, producing low air velocity in this area. Still in this rear zone, the entrainment effect of the diffused air diminishes as one move away from the evaporators, and the minimum air velocity can therefore be observed on this plane near the side walls and in the center. Figures 4-b)- and c)- show the air velocity distribution in the middle and bottom XY planes respectively. Return air flows uniformly through the air channel between the crates. As the temperature in the cold room drops, the cold air becomes denser, and a large volume of it passes at high speed close to the floor.

The average air velocity in the lower, middle and upper planes is 2.48 m/s, 1.34 m/s and 0.87 m/s respectively, while the average velocity for all three planes is 1.56 m/s. The air speed heterogeneity index HI is lowest in the middle and lower planes. In the agricultural preservation zone, a maximum HI of 41.64% was obtained on the median plane, indicating a deviation of 0.64 m/s from the mean velocity. This low HI value on this plane indicates greater uniformity in the velocity distribution. The greatest heterogeneity in velocity distribution is obtained on the upper plane, with an HI value of 222.06%. See Figure 5.

Validation with the Experimental Study

The results obtained experimentally were imported into COMSOL Multiphysics, version 5.3a, so that they could be compared with those of the mathematical model developed. Figures 6 and 7 respectively show a comparison of aeraulic profiles between the simulation tool and experimental results. Analysis of the various curves shows that the discrepancies between calculated and measured mean velocities are small. These deviations can be considered satisfactory in view of the various simulation and experimental parameters influencing model performance, such as variations in experimental inlet air velocity. Our results confirm those of the authors' study (Bishnoi & Aharwal, 2020), which showed that the air velocity distribution in a parallelepiped-type cold store exhibits low heterogeneity on the median and bottom planes. They also reveal greater uniformity of air velocity on the median plane in the agricultural products storage area. The mean relative absolute errors for the calculated and measured mean velocities are presented in Table 1 below.

Conclusion

The mathematical model developed can be used to predict fluid flow in vacuum cold rooms and/or cold rooms loaded with agricultural products. The model equations have been solved and validated using experimental data from a parallelepiped photovoltaic solar cold store. The results of the numerical study confirm those of some authors' experimental studies. The mean relative absolute error for velocity amplitude prediction is around 0.31 on the median plane and 0.15 on the lower plane. Maximum velocity heterogeneity was obtained on the upper plane with an HI value of 222.06%. Such a numerical and experimental study is essential and beneficial for studying aeraulic profiles in the design and operation of cold rooms, but also for understanding the cooling phenomenon in order to optimize the performance of the cold device.

Nomenclatures

u : velocity obtained at a specific position (m/s)

$\bar{u}$: average velocity obtained from different planes (m/s)

V : fluid flow velocity (m/s)

D_H : hydraulic diameter (m)

ν : kinematic viscosity (m^2/s)

ρ : air density ($kg.m^{-3}$)

p : pressure (Pa)

μ : dynamic air viscosity ($kg.m^{-1}s^{-1}$)

μ_t : turbulent viscosity or turbulent eddy (kg.m^{-1}s^{-1})

I : unit tensor

F : volume force due to natural convection (N)

κ : turbulent kinetic energy (m^2/s^2)

ε : turbulent dissipation rate (m^2/s^3)

C_μ : turbulent model coefficient

P_k : turbulent kinetic energy generation term by Reynolds stresses.

σ_k, σ_ε, $C_{\varepsilon 1}$, $C_{\varepsilon 2}$: model constants

Acknowledgments

The authors would like to thank the Laboratoire d'Energies Thermiques Renouvelables (L.E.T.RE) and the Institut de Recherche en Sciences Appliquées et Technologies (IRSAT) for agreeing to monitor this study. The authors also acknowledge the financial support of the Government of Burkina Faso through the Programme d'Appuis à l'Enseignement Supérieur (PAES).

Author Contributions

The co-authors have all contributed to the success of this document. Some helped me with testing and data processing, while others followed and corrected the document as it was being written.

References

Amadou Oumarou, F. (2021). Impact de la nature des matériaux, de l'orientation et de la ventilation sur le confort thermique dans l'habitat individuel en climat sahélien [Thèse de Doctorat Unique]. Joseph KI-ZERBO.

Asmi, A., Putra, J. C. P., & Rahman, I. A. (2013). Simulation of Room Airflow Using Comsol Multiphysics Software. Applied Mechanics and Materials, 465-466, 571-577. https://doi.org/10.4028/www.scientific.net/AMM.465-466.571

Bishnoi, R., & Aharwal, K. R. (2020). Experimental investigation of air flow field and cooling heterogeneity in a refrigerated room. Engineering Science and Technology, an International Journal, 23(6), 1434-1443. https://doi.org/10.1016/j.jestch.2020.05.004

Cardinale, T., Fazio, P., & Grandizio, F. (2016). Numerical and Experimental Computation of Airflow in a Transport Container. International Journal of Heat and Technology, 34(4), 734-742. https://doi.org/10.18280/ijht.340426

COMSOLMultiphysicsTM. (2007). COMSOL multiphysics user's guide. COMSOL Inc, Burlington.

Duret, S., Hoang, H.-M., Flick, D., & Laguerre, O. (2014). Experimental characterization of airflow, heat and mass transfer in a cold room filled with food products. International Journal of Refrigeration, 46, 17-25. https://doi.org/10.1016/j.ijrefrig.2014.07.008

Hoang, H.-M., Duret, S., Flick, D., & Laguerre, O. (2015). Preliminary study of airflow and heat transfer in a cold room filled with apple pallets: Comparison between two modelling approaches and experimental results. Applied Thermal Engineering, 76, 367-381. https://doi.org/10.1016/j.applthermaleng.2014.11.012

Kabore, H., Compaore, R. M. C., Yamba, K., Palm, K., & Sanogo, O. (2024). Two-Dimensional Modelling Of Heat Transfer In The Walls Of A Parallelepiped Cold Room: The Case Of A Transportable Container. International Journal of Engineering Sciences & Research Technology, 13(6). https://doi.org/10.57030/ijesrt.13.6.1.2024

Lewis, R. W., Nithiarasu, P., & Seetharamu, K. N. (2004). Fundamentals of the Finite Element Method for Heat and Fluid Flow (1re éd.). Wiley. https://doi.org/10.1002/0470014164

Moureh, J., Menia, N., & Flick, D. (2002). Numerical and experimental study of airflow in a typical refrigerated truck configuration loaded with pallets. Computers and Electronics in Agriculture, 34(1-3), 25-42. https://doi.org/10.1016/S0168-1699(01)00178-8

Nahor, H. B., Hoang, M. L., Verboven, P., Baelmans, M., & Nicolaï, B. M. (2005). CFD model of the airflow, heat and mass transfer in cool stores. International Journal of Refrigeration, 28(3), 368-380. https://doi.org/10.1016/j.ijrefrig.2004.08.014

Ouedraogo, B. (2017). Conception, Realisation Et Etude Du Fonctionnement En Convection Naturelle D'une Cellule Solaire De Conservation De Produits Agroalimentaires : Application À L'oignon. Université Joseph KI-ZERBO.

Sajadiye, S. M., & Zolfaghari, M. (2017). Simulation of in-line versus staggered arrays of vented pallet boxes for assessing cooling performance of orange in cool storage. Applied Thermal Engineering, 115, 337-349. https://doi.org/10.1016/j.applthermaleng.2016.12.063

Uba, F., Esandoh, E. O., Zogho, D., & Anokye, E. G. (2020). Physical and mechanical properties of locally cultivated tomatoes in Sunyani, Ghana. Scientific African, 10, e00616. https://doi.org/10.1016/j.sciaf.2020.e00616

FIGURES & TABLES

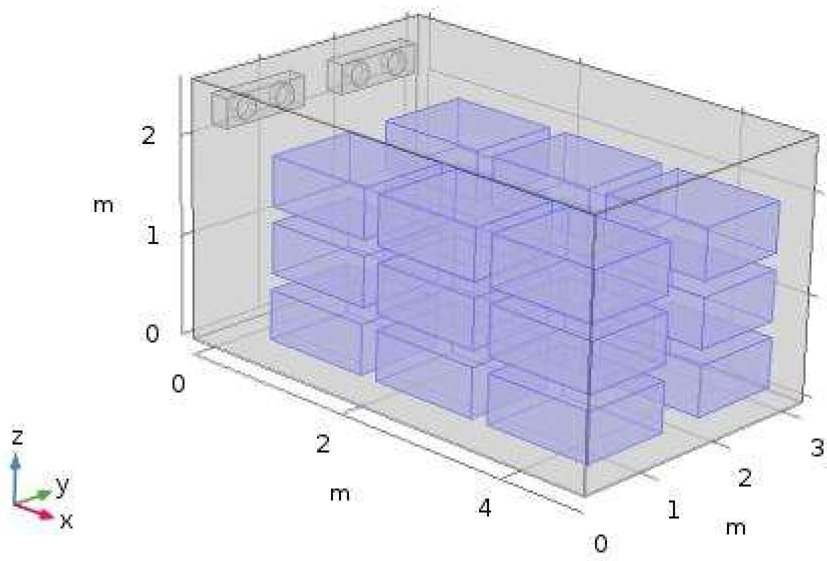

Figure 1: Model of the cold device containing the loaded products

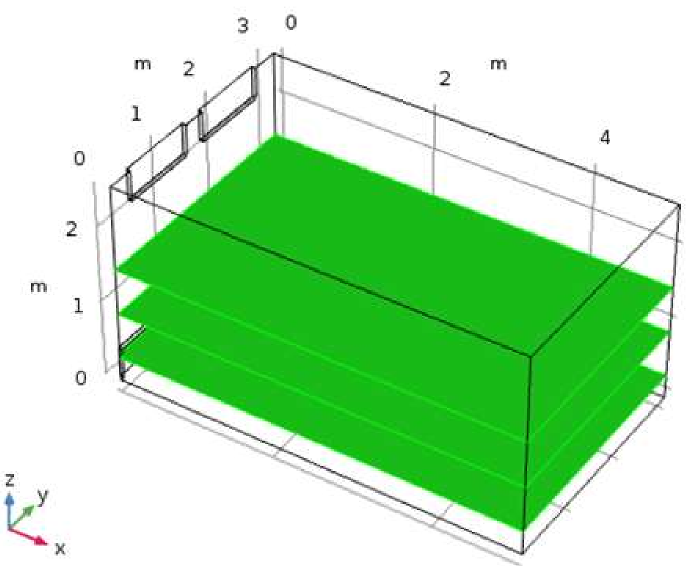

a)_ Three XY planes

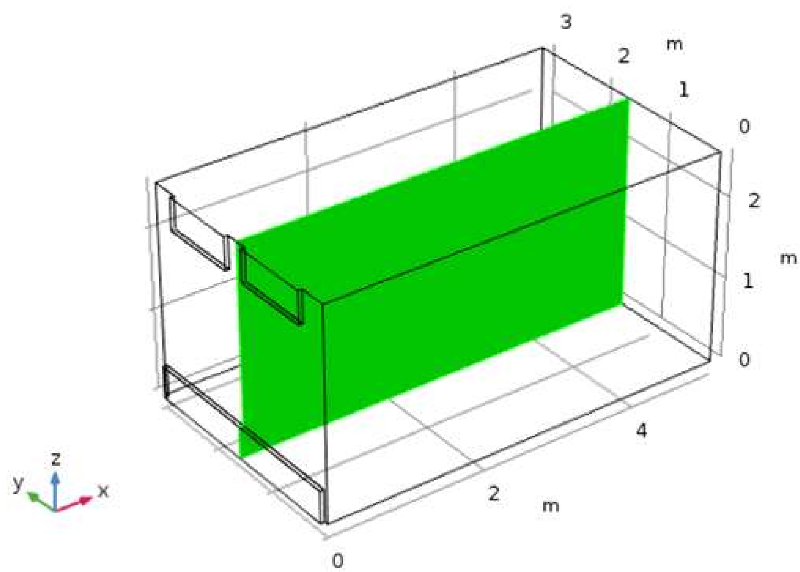

b)_ ZX plane

Figure 2: Presentation of the different planes. a)_ Three XY planes and b)_ Cross-section, ZX plane

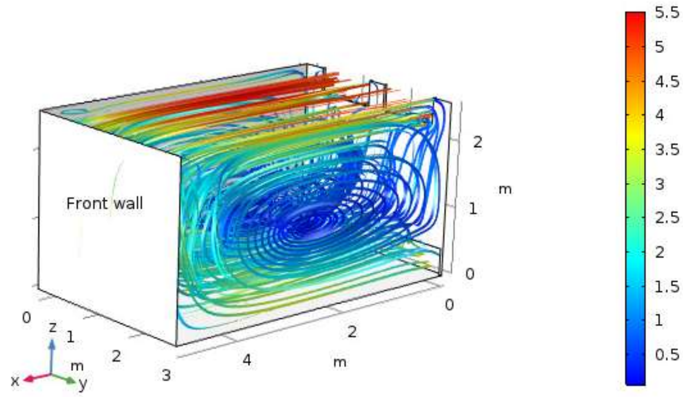

Figure 3: Air velocity distribution streamline

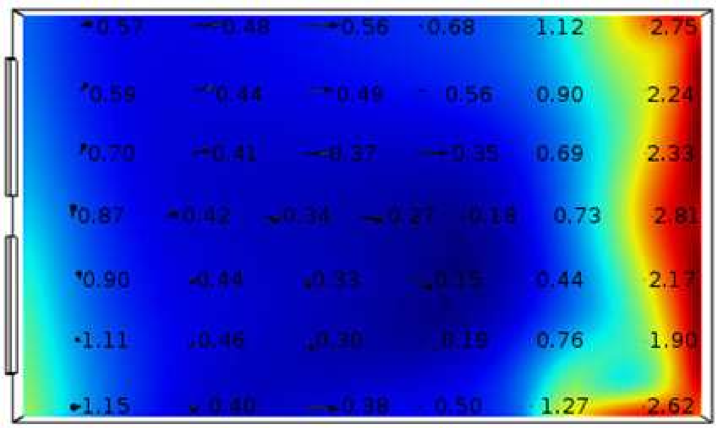

a)_ Top view == Top plane

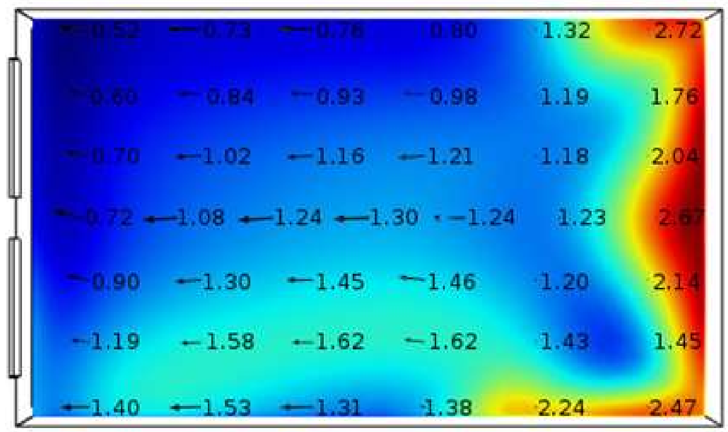

b)_ Top view == Middle plane

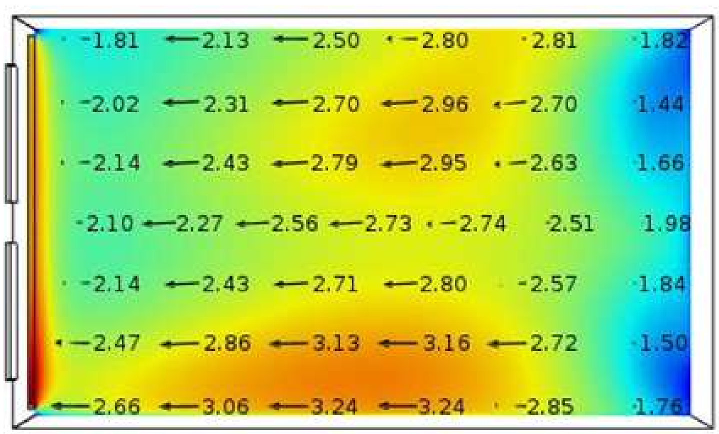

c)_ Top view == Bottom plane

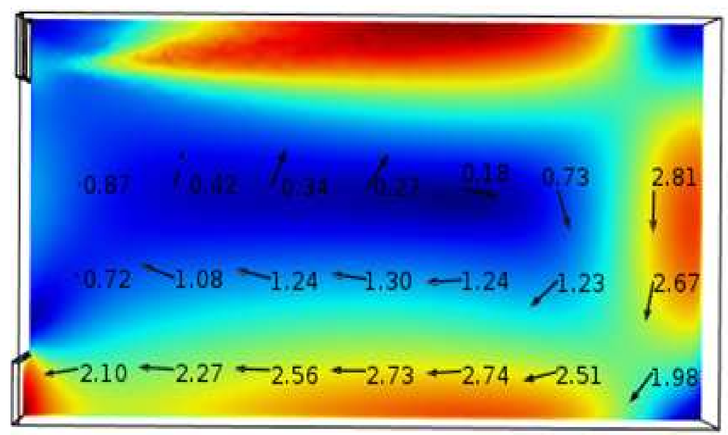

d)_ Side view == Cross section

Figure 4: Air velocity and direction inside the cold room

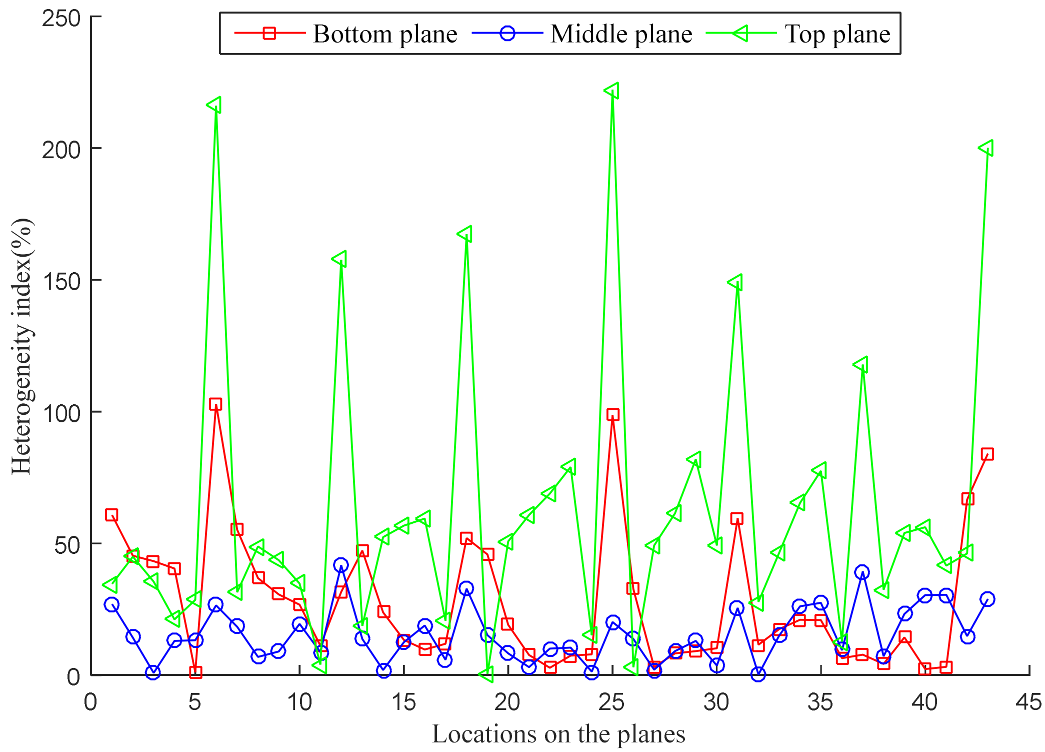

Figure 5: Air velocity heterogeneity index at 43 points on the different planes

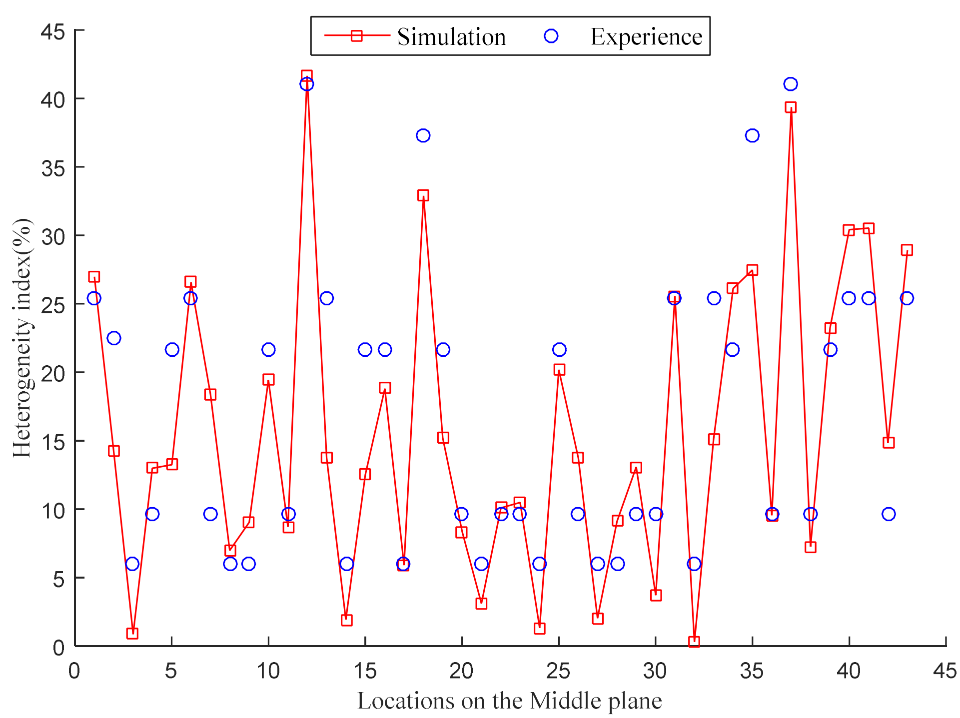

Figure 6: Comparison of simulated and experimental airflow profiles in the middle planes

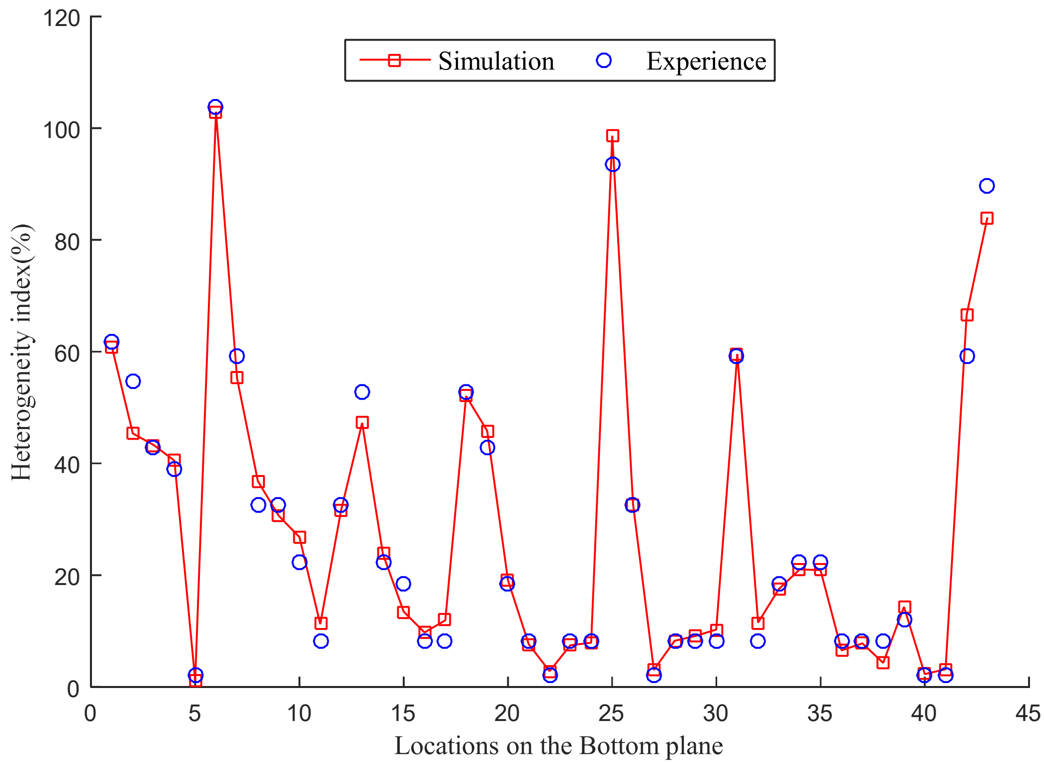

Figure 7: Comparison of simulated and experimental airflow profiles in the lower planes

Table 1: CFD calculation error distribution on different XY planes

Plane	Middle	Bottom
Component (m)	Z = 0.91	Z = 0.31
Calculated average speed (m/s)	1.34	2.48
Measured average speed (m/s)	0.64 ± 0.05	1.03 ± 0.05
$\bar{E}_{CFD}$ (%)	31.1	15.8